Observation of surface roughening on Cu(1, 1, 5)

F. Fabre, D. Gorse, B. Salanon, J. Lapujoulade

J. Physique **48** (1987) 1017-1028 JUIN **1987**, PAGE 1017

Classification
Physics Abstracts
68.20 — 64.70 — 79.20R

Observation of surface roughening on Cu(1, 1, 5)

F. Fabre, D. Gorse, B. Salanon and J. Lapujoulade

Service de Physique des Atomes et des Surfaces, Centre d'Etudes Nucléaires de Saclay, 91191 Gif-sur-Yvette, Cedex, France

(*Reçu le 21 novembre 1986, accepté sous forme définitive le 20 février 1987*)

Résumé. — Nous présentons une analyse détaillée de la topographie de la face de cuivre Cu(1, 1, 5) pour des températures T ; $70\ K < T < 670\ K$. L'analyse de la forme du pic spéculaire de diffraction d'hélium en fonction de la température est en accord avec le modèle de transition rugueuse proposé par Villain *et al.* La température de transition rugueuse est $T_R = 380$ K. A partir de l'anisotropie de la forme des pics, on en déduit l'énergie de répulsion entre marches qui vaut $W_n = 120$ K par maille élémentaire. La procédure expérimentale est détaillée avec soin et ses conséquences sont discutées. La liaison entre rugosité à petite et grande échelle est indiquée.

Abstract. — We present a detailed analysis of the topography of the Cu(1, 1, 5) surface in the temperature range $70\ K < T < 670$ K. The line-shape analysis of the specular helium beam diffraction peak as a function of temperature is found to be in agreement with a model of roughening previously proposed by Villain *et al.* The roughening temperature is found to be $T_R = 380$ K. From the anisotropy of peak profiles, the step repulsive energy is deduced and found to be $W_n = 120$ K per lattice spacing. The experimental procedure is carefully examined and its consequences are discussed. The connection between roughness at small and large scale is indicated.

1. Introduction.

It is now well known that surface defects can have an appreciable effect on the physical properties and chemical reactivity of surfaces. With this in mind, several techniques have been used such as L.E.E.D., electron microscopy and scanning tunnelling microscopy. Due to its high sensitivity to atomic scale features in the uppermost layer helium beam diffraction (H.B.D.) is a very useful tool.

For similar reasons, theoretical work has focused on surface defects. In the beginning of the 50's the concept of a roughening transition of crystal faces has been first developed by Burton, Cabrera and Frank [1]. However it is only in 1980 that the roughening transition of the basal p(0001) plane of hcp He_4 has been observed around 1.2 K [2]. For close-packed metal surfaces, it was generally believed that the roughening temperature is higher than the melting point. Looking at the thermal dependence of H.B.D. peak intensities for stepped (1, 1, n) faces of copper, Lapujoulade *et al.* [3] have proposed in 1983 that the anomalous behaviour observed was indeed due to thermal roughening. A model was then developed by Villain *et al.* [4] (hereafter referred to as V.G.L.). This model generalizes the well known « Solid-On-Solid » model [5] to the anisotropic case of a stepped surface. The model predicts the occurrence of a roughening transition at a finite temperature T_R. It also indicates that above T_R, the shape of the H.B.D. peaks is a power law with respect to the direction parallel or perpendicular to the steps. The power law behaviour has been first confirmed experimentally by Conrad *et al.* [6], who did not measure the anisotropy.

The purpose of this paper is to present a detailed study of diffraction line shapes in both directions. This yields evidence for the roughening of Cu(1, 1, 5) more precisely than in previous publications [3, 4]. But the goal now is more extensive. It will be shown that one can extract important physical quantities which have never been measured before, i.e., the step-step repulsive energy and the kink formation energy. Moreover the limits of the model will appear and the way to generalize it will be introduced.

The outline is as follows : in section 2, we describe the experimental apparatus, crystal orientation and

cleaning procedures. In subsection 3.1, we present experimental evidence for a temperature dependent kink density for Cu(115). In subsection 3.2, we briefly describe the V.G.L. model of roughening and emphasize the approximations in the treatment of scattering. In the calculation of the scattered intensities, we also examine the shape of peaks in relation with their in-phase or out-of-phase character, as evidenced by the oscillatory behaviour of peak widths. Using these results we present the details of our line shape analysis in subsection 3.3. Finally, subsection 3.4 is devoted to discussion and conclusions. Section 4 summarizes our findings and gives perspectives.

2. Experiment.

The experimental set up has been fully described elsewhere [7, 8]. We use a Campargue nozzle beam giving a high intensity molecular flow (10^{20} atoms/steradian), with narrow angular (0.2° from the nozzle) and velocity distribution ($dE/E = 0.06$). The nozzle is held at room temperature and the beam energy is 63 meV. When scattered by the copper sample, surrounded by a 5×10^{-11} Torr background pressure, the He atoms are collected into a stagnation ionization detector sensitive to the helium flux. The incident beam is chopped at low frequency (2.5 Hz) and the signal is detected by a lock-in amplifier. The detector sensitivity is then about $10^{-4}\, I_0$ (I_0 being the incident beam intensity).

The sample is mounted on a three-axis goniometer. The sample temperature, which can be as low as 70 K is measured with a WRe (5 %)/WRE (26 %) thermocouple spot welded on the crystal. Heating is achieved either by radiation or by electron bombardment. The accuracy of temperature measurement is about ± 5 K.

The detector can be rotated about two axes, consequently in-plane as well as out-of-plane scattered intensities can be measured as shown in figure 1. The incident and scattering angles, θ_i and θ_f, are clearly defined. φ_f is not the ordinary azimuthal angle (i.e. in the sample referential) and it is measured in the detector referential. As a consequence, the real peak anisotropy ($\Delta\theta_f/\Delta\varphi_f$) is different from what appears on the curves labelled θ_f and φ_f (cf. Fig. 9). The angular width of the detector is 0.22° (F.W.H.M.).

The (1, 1, 5) face was spark cut from a single crystal along a plane parallel to the (1, $\bar{1}$, 0) direction and tilted by a 15.79° angle with respect to the (1, 0, 0) plane. Previous measurements have shown that the corrugation parallel to the steps is negligible so that the structure is quasi one-dimensional (see Fig. 2).

The preparation of the surface was done as follows : first the sample was desulfurated at 1 173 K for two weeks in a purified H_2 flow. Second it underwent a manual grinding and electro-polishing treatment. Finally, it was carefully cleaned *in situ* by carrying out alternate cycles of argon ion bombardment (Ar^+, 400 V, 10 μA, 1 H), and annealing at 773 K for 15 min prior to the first measurement. The cleanliness was checked by Auger spectrocopy and finally by the diffraction itself which proved to be the most sensitive tool to detect contamination.

In a first series of experiments, the He beam was incident in the direction indicated by the arrow in figure 2, perpendicular to the steps so that the major part of the scattering is concentrated in the incidence plane. In another experiment, the incident beam was parallel to the steps, in this case only the specular beam is located in the incidence plane.

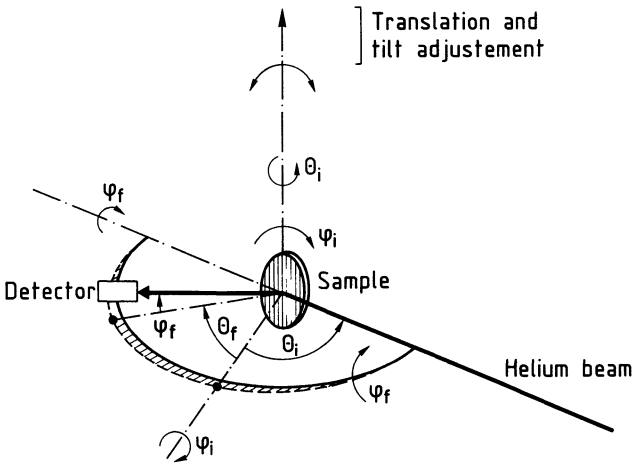

Fig. 1. — Schematic drawing of the experimental design, showing the different angles.

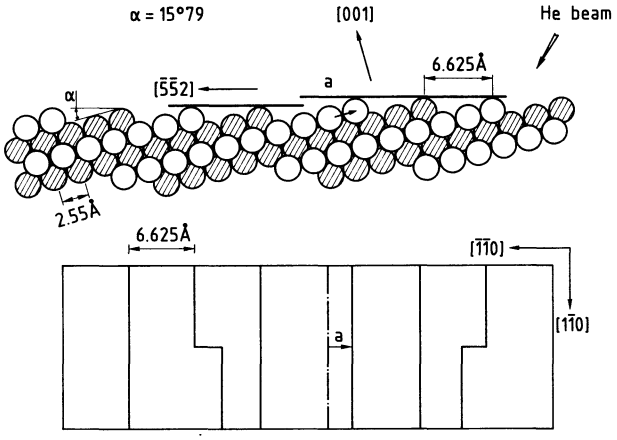

Fig. 2. — Side and top view of a hard sphere model of the Cu(1, 1, 5) surface : a defect step of shift a is shown in the side view, kinks in the terrace edge are shown in the top view.

3. Results.

3.1 Evidence for roughness on Cu(1, 1, 5).

3.1.1 *Diffraction patterns.* — Diffraction patterns for various sample temperatures were obtained. The incident beam was in the ($\bar{5}$, $\bar{5}$, 2) azimuth. Typical results are reported in figure 3. The in-plane scattered intensity I normalized to the incident one, is plotted *versus* the reflection angle θ_f. Figure 3a shows the diffraction spectrum for a sample temperature equal to 70 K. Several diffraction peaks were clearly identified (from ($\bar{7}$, 0) to (2, 0)). Figure 3b shows a diffraction scan for a sample temperature equal to 670 K, where the peaks (2, 0) and (0, 0) are broadened. In the same way, for these broad peaks, the decrease of intensity with temperature is more pronounced than for the narrow peaks, as shown in figure 3. Clearly, at any incident angle we have observed that some peaks are broadened as the temperature is raised while others are not. Moreover, for a given sample temperature the half-width of the specular peak displays some periodicity with the incident angle, as can be seen in figure 4. This behaviour is quite similar to that observed by Conrad *et al.* on Ni(1, 1, 5) [6].

Generally speaking, the increase of intensity in peak tails with sample temperature might be the consequence of inelastic scattering. However the oscillatory behaviour of the peak widths *versus* the incidence shows unambiguously that broadening effects reflect incoherent scattering due to disorder, as discussed below.

Consider the (1, 1, 5) face of f.c.c. lattice which consists of (1, 0, 0) terraces separated by monoatomic steps (see Fig. 2). Thermal properties of the face are presumably fixed by the kink creation energy and by the step-step repulsion energy. At low and medium temperatures (where the creation of adatoms and vacancies on terraces is very unlikely), entropic effects make step edges meander. This leads to local surface shifts as indicated in figure 2. So the surface appears as a patchwork of shifted domains. The result will be interference effects either constructive or destructive according to the value of the momentum transfer. More precisely, the interference condition can be expressed as a function of the momentum transfer in the direction of the displacement of the step, q_x, i.e. parallel to the (1, 0, 0) terrace. For the specular beam the relation can be written :

$$a \,.\, q_x = 2 \,.\, a \,.\, |\mathbf{k}i| \,.\, \cos\,\theta_i \,.\, \sin\,\alpha$$

($\mathbf{k}i$ is the incident momentum, θ_i and α are defined in figs. 1 and 2). The condition which leads to constructive interferences is :

$$a \,.\, q_x = 2\,n \,.\, \pi \qquad (1)$$

where a, the interatomic distance, is the magnitude

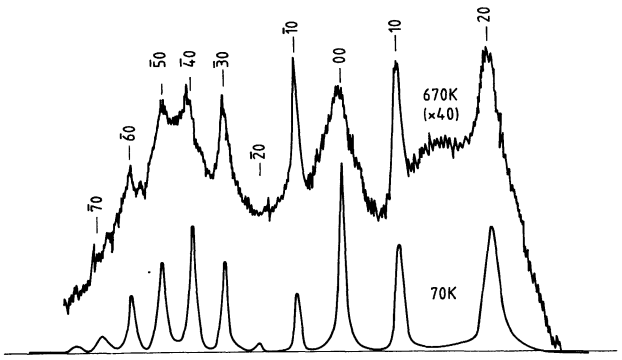

Fig. 3. — In plane scattering intensity relative to the direct beam intensity as function of θ_f. The beam is incident in the ($\bar{5}$, $\bar{5}$, 2) azimuth, $\theta_i = 51°9$, $K_i = 11$ Å^{-1}, $T =$ 70 K and 670 K.

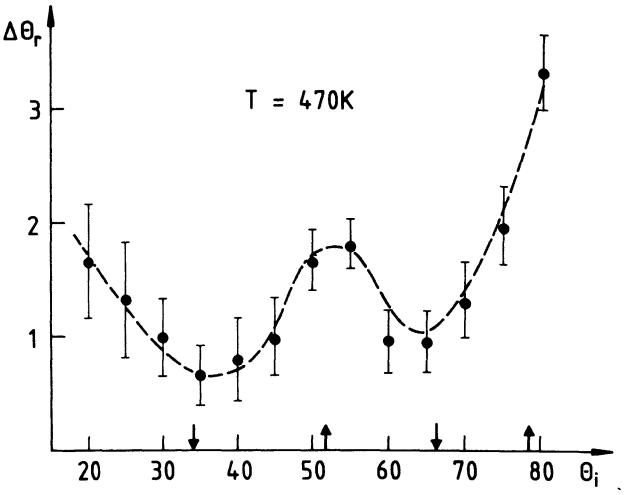

Fig. 4. — Plot of the in-plane widths (F.W.H.M.) *vs.* incidence angle, of the specular peak, $T = 470$ K. Arrows indicate in-phase (↓) and anti-phase (↑) positions as deduced from the crystal geometry. ($\theta_i = 51°9$, ($\bar{5}$, $\bar{5}$, 2) azimuth). $\theta_r = \theta_f$.

of an elementary step shift (see Fig. 2) and n is an integer.

All portions of the Cu(1, 1, 5) surface shifted by integral multiples of a will scatter constructively. These angles were called « Bragg angles » by Conrad *et al.* [6] which may be confusing because all diffraction peaks are centred on Bragg positions for the Cu(1, 1, 5) face. A better name could be « in-phase » peaks or angles, which is currently used in the L.E.E.D. community.

For a momentum transfer q_x satisfying :

$$a \,.\, q_x = (2\,n + 1) \,.\, \pi \,, \qquad (2)$$

portions of the (1, 1, 5) face shifted by integral multiples of a scatter destructively. Under these conditions (anti-phase direction), the peak intensity is reduced and the half-width is increased in a

coupled manner. For anti-phase directions the maximum sensitivity to such a surface disorder is obtained. Minimal and maximal peak widths are experimentally observed in the phase and anti-phase positions predicted by the model and the crystal geometry (arrows in Fig. 4 indicate calculated in-phase and anti-phase positions). The halfwidth variation itself with q_x is discussed in paragraph 3.3, together with the model of roughening.

The peak width evolution with respect to q_x has been measured for different temperatures between 70 K and 670 K. The same periodicity is obtained. Consequently the same kind of disorder is observed in this range of temperature. We want to emphasize here that the simple observation of the period of the peak width oscillations gives strong indications about the type of surface disorder. For instance, one can estimate the influence of disorder on the (1, 0, 0) terraces ; in this case, distinct portions of the Cu(1, 1, 5) face would be shifted by integer multiples of $b = a/\sqrt{2}$ in the direction perpendicular to the terrace. Consequently the phase shift could be written as

$$q_z \cdot b = 2\, b \cdot |ki| \cdot \cos\theta_i \cdot \cos\alpha \,. \qquad (3)$$

In-phase positions would then be given by

$$q_z \cdot b = 2\, n \cdot \pi \,. \qquad (4)$$

Relation (4) is obviously different from (1) and predicts a smaller periodicity which is not observed. Even if disorder on the terraces (energetically less probable) cannot be completely ruled out, the present experimental data prove that the dominant type of defects are kinks on step edges.

Similar observations were made in the out-of-plane direction (width in $d\varphi_f$), for the incident beam in the $(\bar{5}, \bar{5}, 2)$ azimuth.

In the second part of the experiment, the incident beam was in the $(\bar{1}, \bar{1}, 0)$ azimuth. As expected for a one-dimensional corrugation only the specular beam could be observed in the incidence plane. The variation of the specular peak half-width as a function of θ_i qualitatively confirms the observations reported above. As no further information from the specular peak is obtained by changing the incidence plane, we have concentrated our efforts on measurements in the $(\bar{5}, \bar{5}, 2)$ azimuth.

The problem of defects due to the crystal misorientation also has to be underlined. If kinks on step edges were present in a regular pattern, as would be expected from a slight angular orientation error they would lead to extra diffraction spots in the out-of-plane direction. We do not observe such peaks, unlike in the case of Conrad *et al.* [6]. Moreover no fractionary index peaks (which would result from a misorientation in the $(\bar{5}, \bar{5}, 2)$ direction) could be detected. Indeed our crystal was oriented within 0.25° of the (1, 1, 5) plane, leading to one extra step every 300 Å.

In summary, the peak-width oscillation is an evidence for thermal surface disorder, its period gives also information on the kind of disorder : kinks on terrace edges leading to shifted domains as shown in figure 5.

3.1.2 *Debye-Waller effects.* — The variation of the specular intensity with temperature for two incident angles is shown in figure 6. For $\theta_i = 34.6°$ the attenuation of the intensity in logarithmic scale is approximately linear with the sample temperature. The temperature range is large. On the contrary, for $\theta_i = 51.9°$ the thermal attenuation shows a knee around 370 K. For $\theta_i = 34.6°$, condition (1) is fulfilled and the specular peak is in the in-phase position whereas it is in an anti-phase position for $\theta_i = 51.9°$.

The observed intensities can be approximated by

$$I_G = I_G^0\, \gamma_G(T) \exp(-2\, W_G(T)) \,,$$

where I_G^0 is the intensity of the G-th peak extrapolated to 0 K, $\exp(-2\, W_G(T))$ is the Debye-Waller factor due to thermal motion and $\gamma_G(T)$ is a coefficient usually called structural roughening factor [9]. For the specular peak, one can assume that $W_G(T)$ writes as

$$W_G(T) = A \cdot f(T) \cdot T \cdot \Delta k_z^2 \qquad (5)$$

where $f(T)$ is a correction due to the zero point motion, and becomes unity at high temperatures,

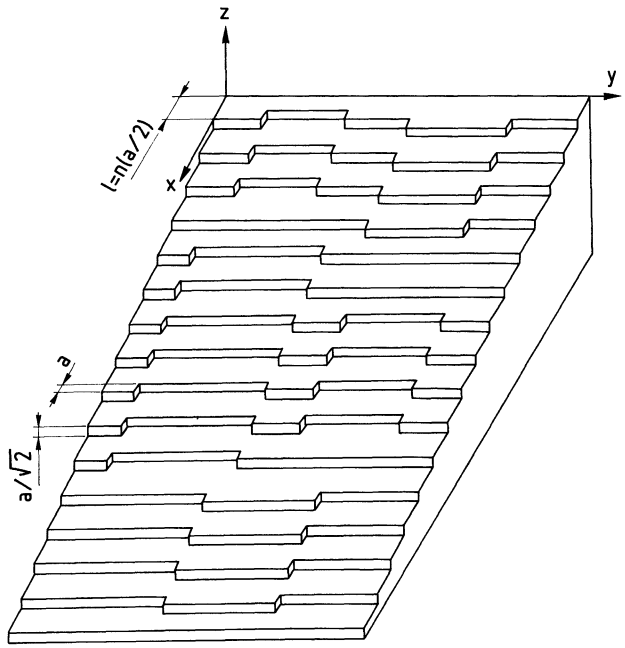

Fig. 5. — Schema of a (1, 1, 5) stepped surface showing domains of constant shift, a is the nearest neighbour atom distance.

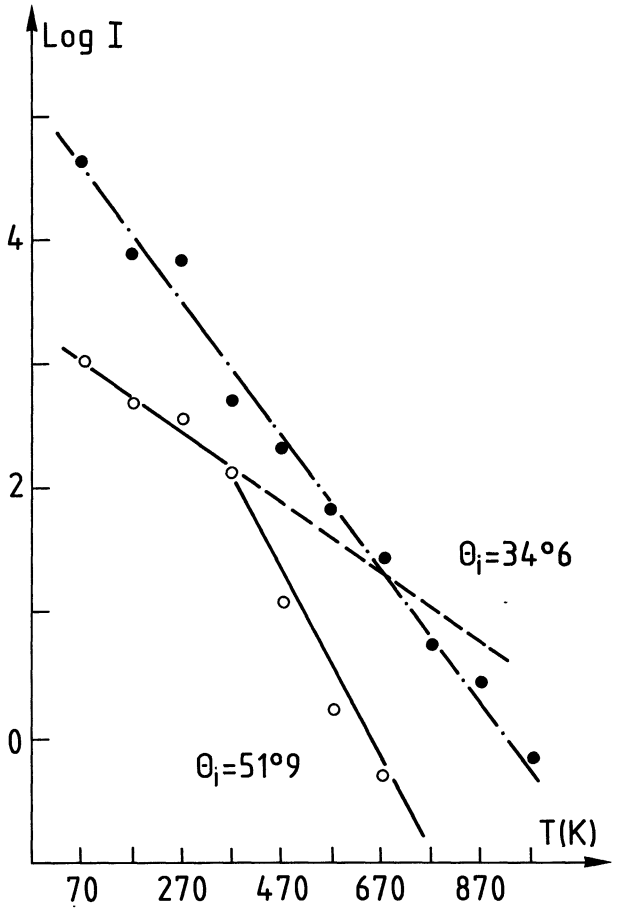

Fig. 6. — Intensity of the specular in plane peaks in the $(\bar{5}, \bar{5}, 2)$ azimuth, for two incidence angle $\theta_i = 34°6$: (in-phase angle), and $\theta_i = 51°9$: (anti-phase angle).

and Δk_z is the momentum transfer perpendicular to the surface including the effect of the attractive well [9]. The $W_G(T)$ factor has been extensively studied for Cu(1, 1, 5) and other Cu faces [9]. We report here measurements for in-phase and anti-phase conditions.

It is shown in the following section that, provided that the domain sizes are large enough, the structure factor $\gamma_G(T)$ is temperature independent for in-phase conditions while it varies for anti-phase conditions. More precisely we show that for the latter case ($\theta_i = 51.9°$) $\gamma_G(T)$ is constant for $T < 370$ K and decreases for higher T, showing the onset of disorder. So $\gamma_G(T)$ gives some insight about surface disorder [4], however, it is a global coefficient and more precise information is found in the analysis of peak shapes [6].

Moreover one can notice that the in-phase condition is favorable for measuring the Debye-Waller factor $2\,W_G(T)$ on stepped surface because in this case the influence of disorder is reduced to a minimum. So we can confirm all previous results obtained in a smaller temperature range [9]. In particular for the specular beam we find for A_{Cu} ($A_{Cu} = A$ in relation (5)) :

$$A_{Cu} = -\,(1.34 + 0.2)\,.\,10^{-5}(\text{Å}^2.\text{K}^{-1})\,.$$

This result has to be related to the value recently obtained by Conrad *et al.* [10] in the similar case of Helium diffraction from Ni(1, 1, 5)

$$A_{Ni} = -\,(7.4 + 1.2)\,.\,10^{-6}(\text{Å}^2.\text{K}^{-1})\,.$$

The ratio of the A coefficients is of interest :

$$R = A_{Cu}/A_{Ni} = 1.81\,.$$

We find that R has exactly the same value as the ratio of the average square displacements of surface atoms $\left(\dfrac{\langle u^2\rangle_{Cu}}{T} \Big/ \dfrac{\langle u^2\rangle_{Ni}}{T}\right)$, which was obtained by calculation [11] for (1, 0, 0) faces.

We also have to emphasize that for Cu(1, 1, 5), using in-phase or anti-phase conditions allows us to separate Debye-Waller effects (phonons) from roughening effects (static disorder) experimentally in an easy manner.

3.2 THE V.G.L. MODEL.

3.2.1 *Calculation of the mean square displacement of the step due to roughening.* — In order to describe the thermal disordering of stepped metal faces, Villain *et al.* [4] studied an anisotropic version of the S.O.S. Model. At zero temperature the crystal face is made of flat terraces separated by straight and equidistant steps. As the temperature is raised, structural defects appear, the model takes into account the predominant ones, i.e. kinks on step edges. The formation of a detour (a step displaced by one interatomic spacing plus two kinks of the ends) involves the formation energy of the two kinks of interest and also the interaction energy of the displaced step with the neighbouring ones. It is assumed that this interaction energy is proportional to the length, L, of the detour. So W can be written as

$$W = 2\,W_0 + LW_n\,.$$

More generally and for any temperature, it is assumed that any disordered configuration can be described in terms of the integer displacement $u_m(y)$ of step m at atom y. By doing so, any roughening of terraces is excluded, which is certainly true for not too high temperatures. For a given configuration described by the function $u_m(y)$ the Hamiltonian of the system is written as

$$\mathcal{H} = \sum_{m,y} W_0(u_m(y+1) - u_m(y))^2 + \sum_{mm'}\sum_{yy'} f(m-m', y-y')(u'_m(y') - u_m(y))\,.$$

The first term reflects the kink contribution ; since for temperatures T lower than W, very few double kinks $(u_m(y+1) - u'_m(y) = \pm 2)$ are expected to occur, this first term is proportional to the total number of kinks. The second term tentatively describes the step-step interaction. This energy is mostly due to elastic forces arising from the lattice strain in the vicinity of a step. So, as the interaction energy between two steps separated by the distance l is proportional to l^{-2}, the energy change when the step is shifted with respect to its neighbouring ones is expected to vary as l^{-4}. Only nearest neighbour interactions are taken into account in the following and $\mathcal{H}$ can be chosen in such a way that the energy W for making a detour is recovered. For instance $\mathcal{H}$ can be written as :

$$\mathcal{H} = \sum_{m,y} W_0(u_m(y+1) - u_m(y))^2 + \\ + \frac{W_n}{2} \sum_{m,y} (u_{m+1}(y) - u_m(0))^2 .$$

This can be seen as an anisotropic Gaussian discrete model. Its critical properties are likely to be the same as those of the Solid-On-Solid Model in an anisotropic version. Although no detailed quantitative solution of such a model is known, it is possible to derive its critical behaviour from a renormalization analysis of a Landau free energy. To this aim an extension of the method developed by Ohta and Kawasaki for the isotropic case has been used [4]. Long wavelength Fourier components of $u_m(y)$ are defined as

$$\tilde{u}_m(y) = \frac{1}{\sqrt{N}} \sum_{\substack{q_x < q_x^c \\ q_y < q_y^c}} u_q \exp(iq_x \cdot m \cdot l + iq_y y)$$

where q_x^c and q_y^c are cut-offs.

Then the free energy can easily be written as [4]

$$F = \frac{1}{2} \sum_q (\eta q_y^2 + \eta' q_x^2) |u_q|^2 + \\ + U(1 - \cos 2\pi \tilde{u}_m(y)) .$$

The first term represents the free energy of a parallel array of elastic lines with a repulsive interaction between each other. As usual the displacements $\tilde{u}_m(y)$ are expressed in terms of a Fourier expansion into normal modes of wave vector q_x and q_y. This array is characterized by two anisotropic excess surface tensions η and η'. This excess surface tension is the difference between the surface tension of a parallel, equidistant array of lines and that of a meandering array. It contains a part due to the increase of line length and a part due to the line repulsion. At a microscopic scale the increase of line length is due to the formation of kinks so that the first part is mainly connected with the kink formation energy W_0 while the second is connected with W_n. In the second term a periodic potential of amplitude U has been introduced in order to account for the discreteness of the displacements along x.

The parameters η, η' and U depend on the physical energies of the microscopic model (W_0, W_n and T). They may be calculated either by renormalizing $\mathcal{H}$ or by simulation.

In a renormalization procedure U tends to a limit U_∞ when q_x^c and q_y^c become vanishingly small. It has been shown that U_∞ vanishes for temperatures T higher than T_R. T_R is the roughening temperature. T_R is defined by the universal relation : $T_R/\sqrt{\eta\eta'} = 2/\pi$. Above T_R the discreteness of $u_m(y)$ is taken into account by renormalizing energetic parameters and using expressions derived assuming continuous $u_m(y)$. One finds that the mean square displacement of step edges diverges logarithmically with distance. This can be written as

$$\langle (u_m(y) - u_0(0))^2 \rangle = \frac{T}{\pi \sqrt{\eta\eta'}} \ln \rho + \text{Cte} \quad (6)$$

with

$$\rho^2 = y^2 \sqrt{\frac{\eta'}{\eta}} + m^2 \sqrt{\frac{\eta}{\eta'}} .$$

Equation (6) is equivalent to the expression obtained by Ohta and Kawasaki [22] for the isotropic S.O.S. model. The anisotropy appears here in the expression of ρ through the factor $\sqrt{\eta'/\eta}$. Moreover, in the limit of strong anisotropy analytic expressions for η and η' can be found [4] for $T_R < T \ll W_0$:

$$\eta = \frac{T}{2} e^{\beta W_0} \quad \eta' = W_n . \quad (7)$$

On the other hand, if renormalization effects are negligible, one would get $\eta = 2W_0$, $\eta' = W_n$. This can be easily seen when deriving the free energy from the discrete Gaussian Hamiltonian and equating it to the above expression of the free energy with $U = 0$.

3.2.2 *Calculation of scattered intensities.* — We first assume that any configuration of steps is composed of domains where $u_m(y)$ is a constant. Moreover we neglect the influence of domain walls on diffraction and the influence of multiple scattering from one domain to the other. Then the total scattered amplitude is the sum of the amplitudes individually scattered by each domain. The diffracted intensity is easily obtained as the product of a form factor I_0 (describing the scattering from the defect free surface and of a structure factor S (describing the correlation of phase between shifted domains). So one can write :

$$I(\Delta K) = I_0(\Delta K)\, S(\Delta K)$$

with

$$S(\Delta K) = \sum_{m,y} e^{i\,\Delta K\,.\,R_{m,y}} \left\langle e^{-i\,\Delta k\,.\,a(u_m(y)-u_0(0))} \right\rangle \quad (8)$$

$\Delta k = (\Delta K, \Delta k_z)$ is the total momentum transfer ; ΔK and Δk_z are the components of Δk respectively parallel and perpendicular to the face ; $R_{m,y}$ is the position of the site denoted by m and y.

$u_m(y)$ is the shift of the step edge at site $R_{m,y}$ and is given by :

$$u_m(y) = u_m(y)\, a$$

where $u_m(y)$ is an integer and a the elementary shift (of length a parallel to the terraces and normal to the steps). Brackets $\langle\ \rangle$ denote a thermal average. We use the Gaussian approximation where the only knowledge of $\langle (u_m(y) - u_0(0))^2 \rangle$ is needed for the calculation of

$$\left\langle e^{-i\,\Delta k\,.\,a(u_m(y)-u_0(0))} \right\rangle .$$

However the discrete nature of the $u_m(y)$'s makes the average periodic with $\Delta k\,.\,a$. Thus one writes :

$$\left\langle e^{-i\,\Delta k\,.\,a(u_m(y)-u_0(0))} \right\rangle = e^{-\langle (u_m(y)-u_0(0))^2 \rangle\, f(\Delta k\,.\,a)} .$$

From the $u \to -u$ invariance of the Hamiltonian, one immediately deduces that of f and one has :

$$f(\varphi) = f(-\varphi) \quad \text{and} \quad f(\varphi + 2\pi) = f(\varphi) .$$

Using a Gaussian distribution for $u_m(y) - u_0(0)$ one finds that to a good approximation f is given by :

$$f(\Delta k\,.\,a) = \pi^2/4(1 - \cos \Delta k\,.\,a) = \\ = \pi^2/4(1 - \cos\,(a\,.\,q_x)) \quad (9)$$

where q_x is defined in relation (1).

The structure factor can be calculated using the logarithmic form of (6).

One then gets :

$$S(\Delta K) = \sum_{\nu=-\infty}^{+\infty} \frac{\Gamma(2-\tau)}{\Gamma\left(\frac{\tau}{2}\right)\Gamma\left(\frac{3}{2}-\frac{\tau}{2}\right)} \times \\ \times \left[(\Delta K_x\, b_x + 2\pi\nu)^2 \sqrt{\eta'/\eta} \right. \\ \left. + (\Delta K_y\, b_y)^2 \sqrt{\eta/\eta'}\right]^{-1+\frac{\tau}{2}}$$

with

$$\tau = \frac{T\pi}{4\sqrt{\eta\eta'}} (1 - \cos\,(\Delta k\,.\,a)) . \quad (10)$$

The variable y was taken to be continuous so that only diffraction peaks within the incidence plane are present. The integer ν denotes the reciprocal lattice vectors so that the intensity is a sum of power laws centred on the Bragg positions. The exponent is $1 - \tau/2$ which varies with the incidence conditions, thus explaining the oscillatory behaviour of peak shapes.

Two neighbouring atoms in a step edge are distant from b_y and two neighbouring steps are separated by b_x. As a special case, when $\Delta k\,.\,a = 2n\pi$ then $\tau = 0$ and the intensity is a Bragg line (phase condition). On the contrary, when one has $\Delta k\,.\,a = (2n+1)\pi$ then τ is maximal and the peak is strongly broadened (antiphase condition).

Equation (9) for the structure factor was established in the case where the face is made of domains of constant u. However, it seems that it is still valid in the more general case of a rough face. Indeed the shape of the intensity in the close vicinity of the Bragg position reflects the long wavelength behaviour of correlation functions, for which it is possible to use the approximation of domains. As far as the short wavelength effects are concerned, their effect is mainly present in peak tails where the influence of the form factor of defects is likely to be predominant.

3.3 LINE-SHAPE ANALYSIS. — The diffraction line-shape is related to the Fourier transform of the correlation function of the phase shifts due to the step displacements (see (8)). As a consequence, line-shape analysis yields more detailed information on the surface structure than the observation of a single parameter such as the peak intensity or peak half-width. Indeed the instrument response function must be taken into account properly in the analysis. Instead of calculating the correlation function by an inversion procedure from the data which necessitates tricky filtering methods, we compute diffracted intensities for various theoretical line-shapes and fit them to the data.

At first, we made comparisons between measured anti-phase line-shapes, and those predicted for different distributions of defects. We used two common distributions, namely an incoherent superposition of finite domains which gives rise to a Gaussian line-shape [12], and a geometric distribution of steps, which gives a Lorentzian line-shape at anti-phase angle [13]. These two functions were convoluted with the instrumental response function. It is beyond doubt that the observed line-shape cannot be fitted neither by Gaussian, nor by Lorentzian forms. The agreement is much better, with an inverse power law function (see Eq. (10)). Figures 7 and 8 show the observed specular line-shape for in-plane scattering at an anti-phase angle with the beam incident in the $(\bar{1}, \bar{1}, 0)$ azimuth for some sample temperatures between 70 K and 570 K.

The procedure for fitting line-shapes to the data is as follows. The incident angle and the azimuth being chosen, we measured the specular intensity, both in and out of the incidence plane. The resulting two scans are then fitted simultaneously in a least square procedure to the theoretical shape. This shape is the

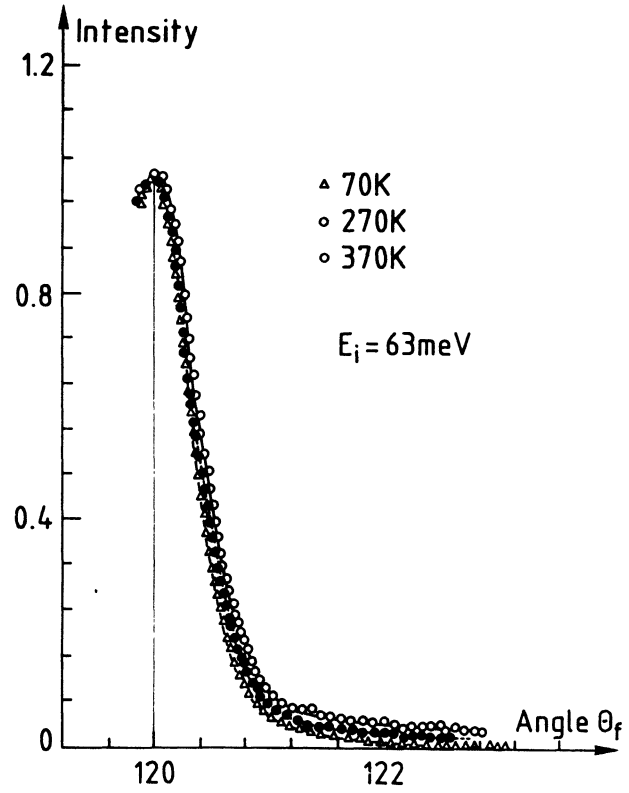

Fig. 7. — Observed specular line-shape for in-plane scattering at anti-phase angle with the beam in the $(\bar{1}, \bar{1}, 0)$ azimuth $\theta_i = 55°$. The crystal temperatures are 70 K, 270 K and 370 K.

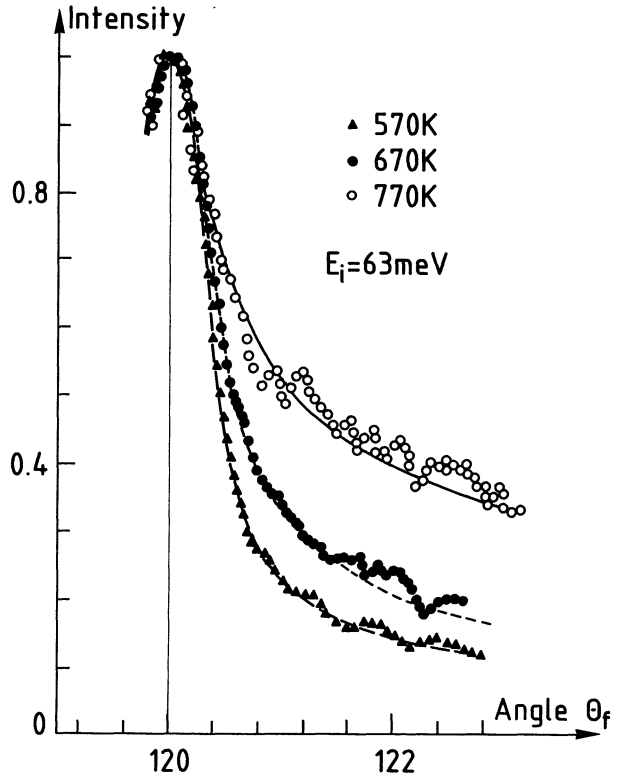

Fig. 8. — Same as for figure 7, the sample temperatures are 570 K, 670 K and 770 K.

spatial convolution of the function defined by equation (10) with the instrumental response function taking into account the incident angular dispersion and the angular detector aperture. For anti-phase conditions the exponent can be taken constant over the angular domain of interest. Consequently we adjust two parameters B_1 and B_2, reflecting respectively the anisotropy and the exponent in a simultaneous fit of two orthogonal intensity scans $B_1 = \sqrt{\eta'/\eta}$ and $B_2 = T \cdot \pi / \sqrt{\eta\eta'} = \tau$. A typical example for $T = 370$ K is shown in figure 9.

The line-shape analysis was carried out only for the specular peak because the calculation is simpler

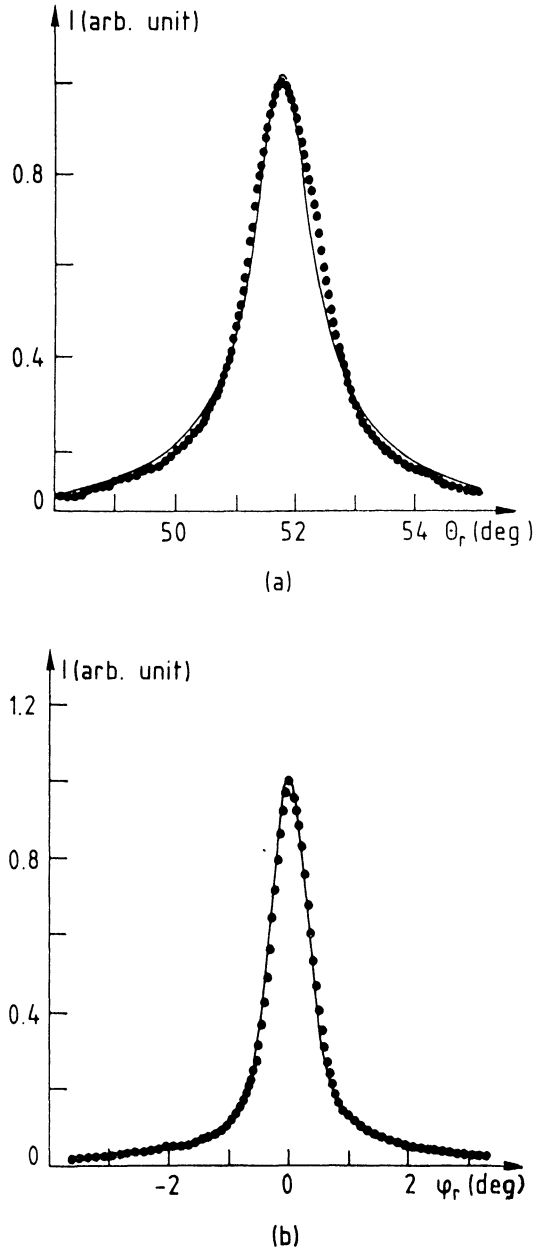

Fig. 9. — Peak profile for He-Cu(115), anti-phase position, $K_i = 11$ Å, $\theta_i = 51°9$, $T = 370$ K. 6a : in-plane profile — 6b : out-of-plane profile. $*$: experimental points. — : fit with (10).

in this case. Moreover studying other peaks would not give more information.

In order to take into account the influence of inelastic scattering and overlap with the tails of neighbouring peaks, we have subtracted from measured intensities a uniform background over the angular distribution for every temperature. Indeed for grazing incidence the inelastic component is broader than for near normal incidence where more appropriate forms would be necessary [14]. The level of the background is deduced from the ratio of the inelastic contribution to the specular peak in the in-phase position.

At first, having chosen the incidence direction which leads to maximum sensitivity to defects ($\theta_i = 51°9$), we determine, for sample temperatures varying from 70 K to 670 K, B_1 and B_2 by the fitting procedure, both with the incident beam in the $(\bar{5}, \bar{5}, 2)$ and $(1, \bar{1}, 0)$ azimuth. The variation of the exponent *versus* temperature is shown in figure 10 from the line-shape of the specular peak with the beam incident in the (5, 5, 2) direction. The anisotropy *versus* temperature is shown in figure 11.

When the incident beam is in the $(1, \bar{1}, 0)$ direction, the specular intensity is very low under anti-phase conditions ($\theta_i = 52°$). This is due to the rainbow pattern. The background and noise are then important. In figure 12, we have shown the value obtained for $\theta_i = 55°$ which is not the strict anti-phase condition, but very close to it. For this angle, the intensity is much higher. Or course $f(q_x)$ — see relation (9) — has to be corrected. The same values of B_1 and B_2 are obtained for the two beam directions, within the experimental uncertainty.

In summary in anti-phase condition and its vicinity, with the incidence plane parallel or perpendicular to steps, all experimental line-shapes even for low temperature (70 K) can be fitted by the power law showing the occurrence of a type of disorder of roughening.

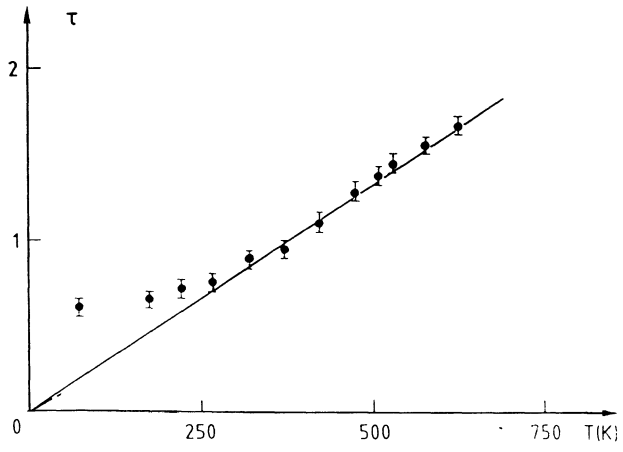

Fig. 10. — Plot of *versus* temperature ($(\bar{5}, \bar{5}, 2)$ azimuth, $\theta_i = 51°9$).

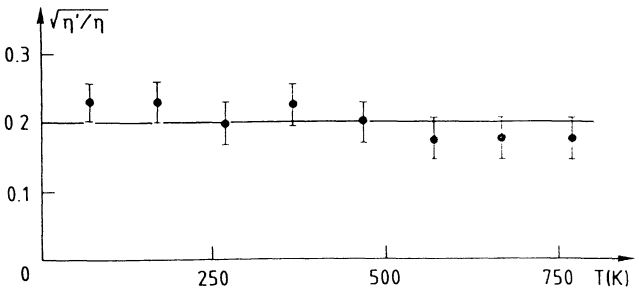

Fig. 11. — Plot of $\sqrt{\eta'/\eta}$ *versus* temperature. The beam is in the $(\bar{5}, \bar{5}, 2)$ azimuth $\theta_i = 51°9$.

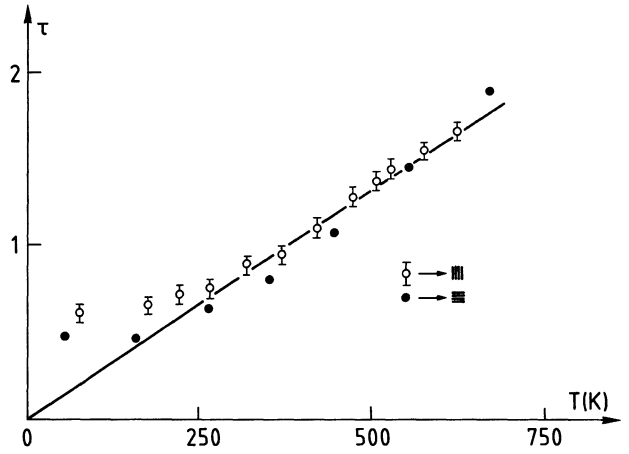

Fig. 12. — Plot of τ *versus* temperature : O corresponds with the beam in the $(\bar{5}, \bar{5}, 2)$ azimuth, $\theta_i = 51°9$ and • : with the beam in the $(\bar{1}, \bar{1}, 0)$ azimuth, $\theta_i = 55°$.

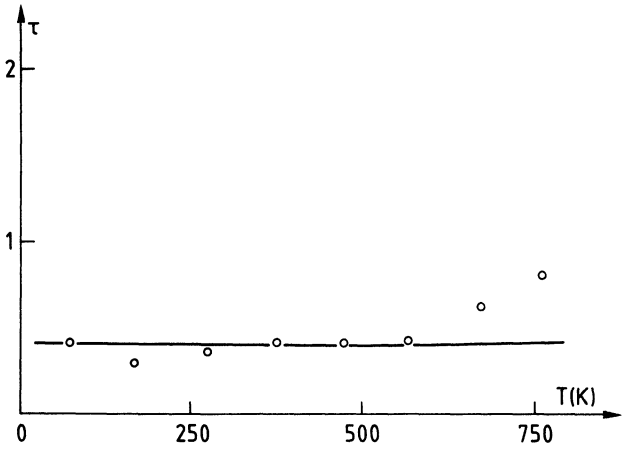

Fig. 13. — Plot of τ *versus* temperature for the in-phase angle, azimuth $(1, \bar{1}, 0)$ $\theta_i = 70°$.

We now examine the case of in-phase conditions. For the exact in-phase condition, expression (10) turns out to be a Delta function. However, experimental data can be fitted by a power-law (10), where τ is now an effective exponent, which represents the average value of τ over the width in q_x of the incident on scattered intensity. Figure 13

gives the value of τ as a function of the sample temperature between 70 K and 770 K. One sees that τ is approximately constant except for high temperatures. For the in-phase condition, in principle, the temperature should not affect the shape of the scattered peak, because the disorder is not seen. Due to the angular width, this condition is not perfectly fulfilled and a slight variation with temperature is observed. Although some problems still remain concerning the exact function [15] for fitting the data, qualitative features such as sharp peaks and weak dependence in temperature are well established.

The third and last point of the line-shape analysis is related to the function $f(q_x)$ itself. Figure 14 shows the plot of τ obtained by fitting the data as a function of q_x. Clearly $f(q_x)$ is proportional to $(1 - \cos(a \cdot q_x))$ (see Eq. (9)).

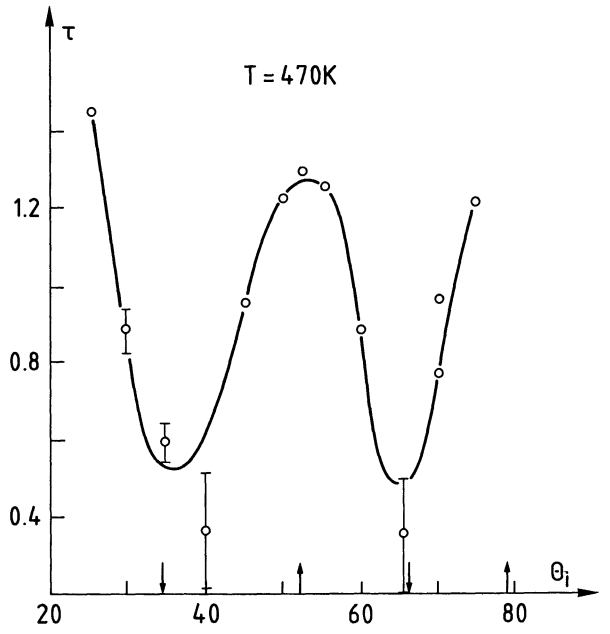

Fig. 14. — $\tau/2$ *versus* the incident angle ($T = 470$ K). Arrows indicate in-phase (↓) and anti-phase (↑) position as deduced from the crystal geometry.

3.4 Discussion.

3.4.1 *Detailed analysis of the experimental proceeding.*

1) Measurement accuracy. — An ideal experiment should be made first with an instrumental width close to zero and second, with the possibility to separate the elastic from the inelastic contribution. The first point is important for the fitting procedure at very low values of q_x and q_y. But in the case of (1, 1, 5) Cu face, the roughness is so high, even at 70 K, that peaks are always broader than the incident beam, both in and out of the incidence plane. In such cases, the anisotropy can be accurately determined ; on the other hand, such measurements are difficult when the broadening is very small. The second point is important for the fitting procedure at very high values of q_x, q_y, and has been fully discussed in reference [16]. A more elaborated procedure for subtracting the inelastic from the elastic diffuse contribution leads to the conclusion that only low-temperature parameters are affected and that the values of the roughness parameter τ are not altered for T above T_R, which is the domain of validity of the theory.

2) Study field. — The analysis of the experimental peak shape is carried out in the vicinity of the specular peak ± 3.5° i.e. for small wave vectors or for long distance correlations ($\rho > 15$ Å). Moreover, due to the instrumental energy and angle spreads, the diffraction pattern is broadened. This angular broadening is correlated to the « transfer width », which is in our case $L_c \simeq 100$ Å. It corresponds to the largest scale, which can be coherently resolved with this instrument. Thus, this experiment allows us to study disorder in a scale 15 Å $< \rho <$ 100 Å. The possibility to separate the elastic from the inelastic contribution and a very good sensitivity have allowed A. M. Lahee *et al.* [17] to study more large-angle diffraction and consequently isolated defects. On the contrary, our study emphasizes the domain statistics on relatively medium and large scales. Figure 15.I shows how one can imagine the sample surface and study field. Moreover we have to keep in mind that the concept of domains is a picture for long and medium wavelength Fourier components of the defect correlation function.

3) Roughness at small and large scale. — The average square shift between two domains, distant about 100 Å (the maximal value one can « see » easily with our instrument) is from relation (6) and for T_R, of the order of one. If we extrapolate the logarithmic law up to the sample size (2 cm) the same quantity would be only of the order of three. This is obviously negligible when compared to the natural roughness of a sample. An examination of the sample with an optical microscope shows random undulations of the surface. Their amplitude is of the order of 0.1 μm for an average wavelength of 0.1 mm (see Fig. 15.II). They are certainly a residue of the original surface after polishing. At any temperature there is a scale L over which the roughness is still frozen. For $T > 300$ K, L is larger than the transfer width (100 Å) and smaller than 0.1 mm (scale of macroscopic roughness). This is why the surface appears to be in thermal equilibrium for $T > 300$ K when analysed by helium diffraction while it remains out of equilibrium even after annealing at 900 K when looked at with a microscope. This frozen equilibrium has been recently studied theoretically by Villain [20], and dynamic properties near the roughening transition by Nozières *et al.* [21].

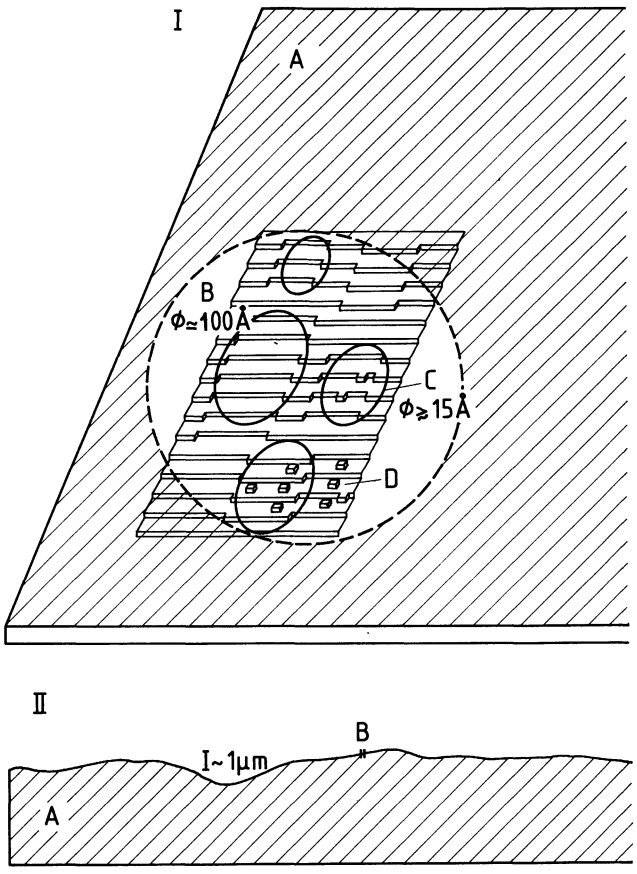

Fig. 15. — Schematic view showing : I - A : a part of the sample. B : the transfer domain, analysed by the He beam experiment ; the diameter is of order of 100 Å. C : the shifted step domains well studied by this experiment ; their sizes are more than 15 Å. D : kinks, adatoms and vacancies which could analyse in a very large angle around diffraction peaks. II - Schematic side view of the sample showing (not at the large scale roughness and the transfer domain).

3.4.2 *Comparison with the V.G.L. model.* — We have shown that the peak profiles for every sample temperature are found to be in good agreement with the model previously proposed by V.G.L. At first, the diffraction peaks are broadened by the step disorder according to a power law. This is the direct consequence of the logarithmic form of the correlation function and this form is the signature of the roughening transition.

The second point is the following : the exponent shows periodic oscillations as a function of q_x. This simply reflects the constructive or destructive interferences between domains of an unperturbed lattice displaced one with respect to the other by one interatomic distance as shown in figure 5.

More precisely, the characteristic roughening temperature is given by $\tau = 1$, in anti-phase condition. We thus deduce from the data that $T_R = 380$ K. This value is discussed in reference [18], in relation with the roughening temperature obtained for Ni(1, 1, 5) face [6] and [16].

The model predicts that the surface roughness should be zero at zero temperature. It is clear from figure 10 that this is not the case. We have previously shown [19] that the surface at low temperature is frozen, in a disorder state corresponding to $T \approx 300$ K. Thus only the linear behaviour of τ for $T > 300$ K is the equilibrium behaviour.

From the value of τ and the anisotropy parameter $\sqrt{\eta'/\eta}$, we can deduce $\eta' = 120 \pm 20$ K and $\eta = 3\,000 \pm 500$ K. According to the V.G.L. model, η' can be identified with W_n, the interaction energy between steps. Thus one gets $W_n \approx 100$ K. We have to underline that this is the first experimental measurement of the interaction energy between steps. As far as η is concerned, the V.G.L. Model predicts that it should be temperature dependent. Fitting the experimental values of τ, for high T, and using the V.G.L. model, we give a value for W_n which is incoherent with that deduced from the anisotropy (Fig. 16). Thus this result of V.G.L. is clearly not supported by the present data. Freezing at low temperatures and the limited range of temperatures can explain this discrepancy. Moreover the value of η, given by V.G.L. is obtained in a one-dimensional approximation which may prove questionable in our case. Indeed the observed logarithmic law is the signature of a strong two-dimensional behaviour.

On the other hand, if renormalization is neglected, one simply gets $\eta = 2\,W_0 \rightarrow W_0 = 1\,500$ K. A rough estimation of W_0 in terms of a broken bond model gives $W_0 = 3\,400$ K. But a more refined estimation which takes band effects into account, leads to

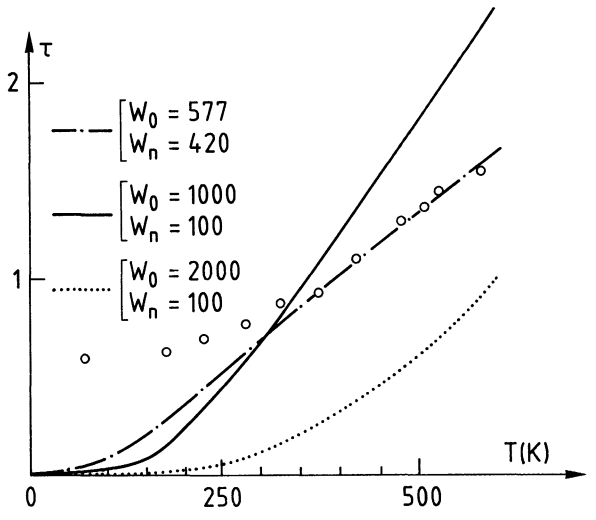

Fig. 16. — τ *versus* temperature ($(\bar{5}, \bar{5}, 2)$ azimuth, $\theta_i = 51°\,9$) experimental points, and the lines are using $\tau = T \cdot \pi / \sqrt{\eta\eta'}$, with $\eta = W_n$ and

$$\eta' = T/2 \exp(W_0/kT) .$$

—·— : one part of the curve is fitted, but W_n and W_0 are unrealistic. — and ··· : W_n, W_0 are more realistic but the lignes disagree with the experimental points.

$W_0 = 2\,300$ K [4]. The value estimated from the data is not too far from those values which are generally assumed to be overestimates. However an exact solution of the model is necessary in order to get a reliable estimate of W_0. This question is open.

Concluding this comparison, it seems that if the surface tension parameters η, and η', are easily settled from the experimental data, more sophisticate models and calculations are needed for the microscopic parameters, such as W_n and W_0.

4. Conclusion.

The main conclusion is (it is now proved both experimentally and theoretically), that metal vicinal surfaces undergo a roughening transition. Helium beam diffraction appears to be a very powerful tool to study such surface thermal disorder. The line-shape analysis allows us to reach the physics of defects which is resumed in 3 parameters : $B_1 = \sqrt{\eta'/\eta}$, which is the measure of the peak anisotropy and the ratio between the two surface tensions, $B_2 = \tau$ which is related to the measurement of the number of thermal defects, and finally the incidence variation of the peak width, which is connected to the type of disorder. This leads to rough estimates of microscopic quantities which were not previously known, namely the kink formation energy and the step interaction energy, but further more accurate theoretical analyses of the model are needed to obtain more reliable values.

We have to underline that these studies have an interest beyond the determination of fundamental parameters. We have also shown that the surface at very low temperatures is frozen and disordered. This fact, allows us now to understand, why diffraction spectra from stepped faces such as Cu(1, 1, 5) and Cu(1, 1, 7) could only be poorly fitted by theoretical calculations. In the analysis of the experimental data peak, intensities were corrected for the instrumental broadening but not for disorder broadening.

These roughness studies are very promising and should stimulate both theoretical and experimental studies.

Acknowledgments.

We gratefully acknowledge M. Lefort, Y. Lejay and E. Maurel for their technical assistance and G. Armand and J. R. Manson for illuminating discussions.

References

[1] BURTON, W. K., CABRERA, N. and FRANK, F. C., *Philos. Tran. R. Soc. London* **243 A** (1951) 299.

[2] BALIBAR, S. and CASTAING, B., *J. Physique Lett.* **41** (1980) L-329.

[3] LAPUJOULADE, J., PERREAU, J. and KARA, A., *Surface Sci.* **129** (1983) 59.

[4] VILLAIN, J., GREMPEL, D. R. and LAPUJOULADE, J., *J. Phys. F: Metal. Phys.* **15** (1985) 809.
See also BLATTER, G., *Surface Sci.* **145** (1984) 419.

[5] WEEKS, J. D., in : *Ordering in strongly fluctuating condensed matter systems,* Tormod Riste Editor (Plenum press, New York) 1980, 299.

[6] CONRAD, E., ATEN, R., KAUFMAN, D., ALLEN, L., ENGEL, T., DEN NIJSS, M., RIEDEL, E. K., *J. Chem. Phys.* **84** (1986) 1015.

[7] LEJAY, Y., LAPUJOULADE, J. and ARMAND, G., *J. Phys. Appl.* **8** (1973) 2070.

[8] LAPUJOULADE, J. and LEJAY, Y., *J. Chem. Phys.* **63** (1975) 1389.

[9] LAPUJOULADE, J., PERREAU, J. and KARA, A., *Surface Sci.* **129** (1983) 59.

[10] CONRAD, E. H., KAUFMAN, D. S., ALLEN, L. R., ATEN, R. M. and ENGEL, T., *J. Chem. Phys.* **83** 10 (1985) p. 5286.

[11] MASRI, P., DOBRZYNSKI, L., *Surface Sci.* **32** (1972) 623.

[12] LU, T. M. and LAGALLY, M. G., *Surface Sci.* **120** (1982) 47.

[13] LAPUJOULADE, J., *Surface Sci.* **108** (1981) 526.

[14] ARMAND, G., private communication.

[15] SALANON, B. and ARMAND, G., in preparation.

[16] CONRAD, E. H., ENGEL, T., ALLEN, L. R., BLANCHARD, D. L. and ENGEL, T., *J. Chem. Phys.* (to be published) and DEN NIJS, M., RIEDEL, E. N., CONRAD, E. H. and ENGEL, T., erratum in *P.R.L.* **57** (1986) 1279.

[17] LAHEE, A. M., MANSON, J. R., TOENNIES, J. P. and WÖLL, Ch., *P.R.L.* **57** (1986) 471.

[18] FABRE, F., GORSE, D., LAPUJOULADE, J. and SALANON, B., *Europhys. Lett.* (in press).

[19] FABRE, F., GORSE, D., SALANON, B. and LAPUJOULADE, J., *Surface Sci.* **175** (1986) L-693-700.

[20] VILLAIN, J., *Europhys. Lett.* **2** (7) (1986) 531-537.

[21] NOZIÈRES, P., GALLET, F. (to be published).

[22] OHTA, T. and KAWASAKI, K., *Prog. Theor. Phys.* **60** (1978) 365.